Research Article | Vol. 26, No. 13 | 25 Jun 2018 | OPTICS EXPRESS 16333
Optics EXPRESS

Propagation properties of Hermite non-uniformly correlated beams in turbulence

JIAYI YU,[1,2] FEI WANG,[2] LIN LIU,[2] YANGJIAN CAI,[2,3,4] AND GREG GBUR[1,5]

[1] *Department of Physics and Optical Science, University of North Carolina at Charlotte, Charlotte, NC 28223, USA*
[2] *College of Physics, Optoelectronics and Energy and Collaborative Innovation Center of Suzhou Nano Science and Technology, Soochow University, Suzhou 215006, China*
[3] *Center of Light Manipulations and Applications, College of Physics and Electronics, Shandong Normal University, Jinan 250014, China*
[4] *yangjiancai@suda.edu.cn*
[5] *gjgbur@uncc.edu*

Abstract: We study the propagation properties (intensity, degree of coherence and scintillation) of a new class of beams in a turbulent atmosphere, which are called Hermite non-uniformly correlated (HNUC) beams. The results show that the beams not only have lower scintillation but also higher intensity than Gaussian-Schell model (GSM) beams over certain propagation ranges. We can adjust the beam order of HNUC beams to enhance the intensity of the beam in the receiver plane and, simultaneously, reduce the detrimental scintillation, and we can also adjust the coherence length of HNUC beams to optimize the effects of a given propagation distance between a signal transmitter and a receiver.

OCIS codes: (030.0030) Coherence and statistical optics; (010.1300) Atmospheric propagation.

References and links

1. L. C. Andrews and R. L. Phillips, *Laser Beam Propagation through Random Media* (SPIE, 2005).
2. J. C. Leader, "Intensity fluctuations resulting from partially coherent light propagating through atmospheric turbulence," J. Opt. Soc. Am. **69**(1), 73–84 (1979).
3. R. L. Fante, "Intensity fluctuations of an optical wave in a turbulent medium: effect of source coherence," Opt. Acta **28**(9), 1203–1207 (1981).
4. V. A. Banakh and V. M. Buldakov, "Effect of the initial degree of spatial coherence of a light beam on intensity fluctuations in a turbulent atmosphere," Optics and Spectroscopy **55**, 423–426 (1983).
5. V. A. Banach, V. M. Buldakov, and V. L. Mironov, "Intensity fluctuations of a partially coherent light beam in a turbulent atmosphere," Optics and Spectroscopy **54**, 626–629 (1983).
6. O. Korotkova, L. C. Andrews, and R. L. Phillips, "Model for a partially coherent Gaussian beam in atmospheric turbulence with application in Lasercom," Opt. Eng. **43**(2), 330–341 (2004).
7. G. P. Berman, V. N. Gorshkov, and S. V. Torous, "Scintillation reduction for laser bames propagating through turbulent atmosphere," J. Phys. B. **44**(5), 055402 (2011).
8. G. Gbur, "Partially coherent beam propagation in atmospheric turbulence," J. Opt. Soc. Am. A **31**(9), 2038–2045 (2014).
9. G. Gbur and E. Wolf, "Spreading of partially coherent beams in random media," J. Opt. Soc. Am. A **19**(8), 1592–1598 (2002).
10. T. Shirai, A. Dogariu, and E. Wolf, "Mode analysis of spreading of partially coherent beams propagating through atmospheric turbulence," J. Opt. Soc. Am. A **20**(6), 1094–1102 (2003).
11. Y. Yuan and Y. Cai, "Scintillation index of a flat-topped beam array in a weakly turbulent atmosphere," J. Opt. **13**(12), 125701 (2011).
12. F. Wang, X. Liu, L. Liu, Y. Yuan, and Y. Cai, "Experimental study of the scintillation index of a radially polarized beam with controllable spatial coherence," Appl. Phys. Lett. **103**(9), 091102 (2013).
13. F. Wang, Y. Cai, H. T. Eyyuboğlu, and Y. Baykal, "Twist phase induced reduction in scintillation of a partially coherent beam in turbulent atmosphere," Opt. Lett. **37**(2), 184–186 (2012).
14. X. Liu, Y. Shen, L. Liu, F. Wang, and Y. Cai, "Experimental demonstration of vortex phase-induced reduction in scintillation of a partially coherent beam," Opt. Lett. **38**(24), 5323–5326 (2013).
15. Y. Yuan, X. Liu, F. Wang, Y. Chen, Y. Cai, J. Qu, and H. T. Eyyuboglu, "Scintillation index of a multi-Gaussian Schell-model beam in turbulent atmosphere," Opt. Commun. **305**, 57–65 (2013).

#330299 https://doi.org/10.1364/OE.26.016333
Journal © 2018 Received 26 Apr 2018; revised 28 May 2018; accepted 31 May 2018; published 13 Jun 2018

Optics EXPRESS

16. O. Korotkova, S. Avramov-Zamurovic, C. Nelson, R. Malek-Madani, Y. Gu, and G. Gbur, "Scintillation reduction in multi-Gaussian Schell-model beams propagating in atmospheric turbulence," Proc. SPIE **9224**, 92240M (2014).
17. Y. Gu and G. Gbur, "Scintillation of pseudo-Bessel correlated beams in atmospheric turbulence," J. Opt. Soc. Am. A **27**(12), 2621–2629 (2010).
18. X. Liu, J. Yu, Y. Cai, and S. A. Ponomarenko, "Propagation of optical coherence lattices in the turbulent atmosphere," Opt. Lett. **41**(18), 4182–4185 (2016).
19. F. Gori and M. Santarsiero, "Devising genuine spatial correlation functions," Opt. Lett. **32**(24), 3531–3533 (2007).
20. F. Gori, V. Ramírez-Sánchez, M. Santarsiero, and T. Shirai, "On genuine cross-spectral density matrices," J. Opt. A: Pure Appl. Opt. **11**(8), 085706 (2009).
21. H. Lajunen and T. Saastamoinen, "Propagation characteristics of partially coherent beams with spatially varying correlations," Opt. Lett. **36**(20), 4104–4106 (2011).
22. Z. Tong and O. Korotkova, "Nonuniformly correlated light beams in uniformly correlated media," Opt. Lett. **37**(15), 3240–3242 (2012).
23. Y. Gu and G. Gbur, "Scintillation of nonuniformly correlated beams in atmospheric turbulence," Opt. Lett. **38**(9), 1395–1397 (2013).
24. X. Jia, M. Tang, and D. Zhao, "Propagation of electromagnetic non-uniformly correlated beams in the oceanic turbulence," Opt. Commun. **331**, 1–5 (2014).
25. Z. Tong and O. Korotkova, "Electromagnetic nonuniformly correlated beams," J. Opt. Soc. Am. A **29**(10), 2154–2158 (2012).
26. Z. Mei, Z. Tong, and O. Korotkova, "Electromagnetic non-uniformly correlated beams in turbulent atmosphere," Opt. Express **20**(24), 26458–26463 (2012).
27. H. Lajunen and T. Saastamoinen, "Non-uniformly correlated partially coherent pulses," Opt. Express **21**(1), 190–195 (2013).
28. C. Ding, Y. Cai, Y. Zhang, H. Wang, Z. Zhao, and L. Pan, "Stochastic electromagnetic planewave pulse with non-uniform correlation distribution," Phys. Lett. A **377**(25-27), 1563–1565 (2013).
29. I. Toselli, L. C. Andrews, R. L. Phillips, and V. Ferrero, "Angle of arrival fluctuations for free space laser beam propagation through non-Kolmogorov turbulence," Proc. SPIE **6551**, 65510E (2007).
30. I. Toselli, L. C. Andrews, R. L. Phillips, and V. Ferrero, "Free-space optical system performance for laser beam propagation through non-Kolmogorov turbulence," Opt. Eng. **47**(2), 026003 (2008).

1. Introduction

In the past decades, a great deal of attention has been paid to the propagation characteristics of optical beams in the turbulent atmosphere owing to their important role in laser radar systems, remote sensing and free-space optical (FSO) communication systems [1]. When a laser beam propagates through atmospheric turbulence, it experiences several deleterious effects, such as excessive beam spreading, beam wander, scintillation (i.e., intensity fluctuation) and angle-of-arrival fluctuation, caused by random variations in the refractive index. Scintillation, as one of the most limiting effects of atmospheric turbulence, reduces the capacity of laser radar systems, remote sensing and FSO systems. Thus it is imperative to take action to mitigate or overcome this effect.

It is well-known that partially coherent beams (PCBs) can have lower turbulence-induced scintillation than their fully coherent counterparts [2–8]. The physical mechanism for the resistance of PCBs to turbulence can be explained from the point of view of the coherent mode representation [9, 10]. Up to now, many papers have studied strategies to reduce the scintillation in turbulent atmosphere by using different kinds of PCBs, e.g., PCBs with special beam profiles [11], states of polarization [12], phases [13, 14] or non-conventional correlation functions (non-Gaussian distribution of the degree of coherence (DOC)) [15–18]. The options listed above, however, just reduce the scintillation, and both high average received intensity and low scintillation are desired when a laser beam is used in FSO communications. Most PCBs considered have had a homogeneous (Schell-model) degree of coherence, and for such beams a decrease of intensity is typical as well.

Since a new method for designing novel correlation functions of scalar and vector PCBs was discussed by Gori *et al.* [19, 20], a great deal of attention has been paid to investigating novel correlation functions of PCBs. In 2011, Lajunen *et al.* introduced a new class of PCBs with a spatially variant correlation function (i.e., nonuniformly correlated (NUC) beams) [21]. Their

Optics EXPRESS

new class was shown to exhibit self-focusing and self-shifting propagation properties. Over the next few years, researchers investigated in detail the evolution of its spectral density [22–28]. Gu *et al.* studied the scintillation of NUC beams in the turbulent atmosphere and showed that such NUC beams not only have lower scintillation but also higher intensity than Gaussian-Schell model beams over certain propagation distances [23]. However, Those promising beams only had a single parameter to vary, namely the spatial correlation length. Here we introduce a new infinite class of beams in which both mode order and correlation length may be changed to adjust the scintillation and focal length.

2. Theoretical model for HNUC beams

Typically, the spatial coherence properties of scalar PCBs are described by either the mutual intensity in the space-time domain or the cross-spectral density (CSD) in space-frequency domain. Both of these functions have to be nonnegative definite kernels. In recent years, the CSD has become the quantity of choice for studying quasi-monochromatic fields. The CSD of the field at the source plane is defined as a two-point correlation function:

$$W(\mathbf{r}_1, \mathbf{r}_2) = \langle E^*(\mathbf{r}_1) E(\mathbf{r}_2) \rangle, \tag{1}$$

where $E(\mathbf{r})$ denotes the field fluctuating in a direction perpendicular to the z axis, and the angular brackets denotes an average over a monochromatic ensemble. We will work at a single frequency ω and suppress its explicit depiction in the arguments of W and E. To be a mathematically genuine correlation function, the CSD must correspond to a nonnegative definite kernel, which is fulfilled if the function can be written in the following form [19],

$$W(\mathbf{r}_1, \mathbf{r}_2) = \int p(v) V_0^*(\mathbf{r}_1, v) V_0(\mathbf{r}_2, v) \, dv, \tag{2}$$

where V_0 is an arbitrary kernel and p is a non-negative function.

For the NUC beams introduced by Lajunen *et al.*, the p and V_0 are defined for a one-dimensional source as [21]

$$p(v) = \left(\pi a^2\right)^{-1/2} \exp\left(-v^2/a^2\right), \tag{3}$$

$$V_0(x, v) = \exp\left(-\frac{x^2}{w_0^2}\right) \exp\left[-ik(x - x_0)^2 v\right], \tag{4}$$

where a is a positive real constant, $k = 2\pi/\lambda$ is the wave number and w_0 is the beam width and x_0 is a real constant.

We introduce a generalized set of higher-order two-dimensional sources with

$$p(v) = (4\pi)^{-1/2} \left(\frac{2}{a}\right)^{2m+1} v^{2m} \exp\left(-\frac{v^2}{a^2}\right), \tag{5}$$

where m is the beam order, and we set V_0 as

$$V_0(\mathbf{r}, v) = \exp\left(-\frac{\mathbf{r}^2}{w_0^2}\right) \exp\left(-ikv\mathbf{r}^2\right). \tag{6}$$

Substituting Eqs. (5) and (6) into Eq. (2), we readily obtain the following expression for the CSD of the generated partially coherent beam:

$$W(\mathbf{r}_1, \mathbf{r}_2) = \exp\left(-\frac{\mathbf{r}_1^2 + \mathbf{r}_2^2}{w_0^2}\right) \mu(\mathbf{r}_1, \mathbf{r}_2), \tag{7}$$

Optics EXPRESS

where $\mu(\mathbf{r}_1, \mathbf{r}_2)$ represents the DOC of the generated beam and is given by

$$\mu(\mathbf{r}_1, \mathbf{r}_2) = G_0 H_{2m}\left(\frac{\mathbf{r}_2^2 - \mathbf{r}_1^2}{r_c^2}\right) \exp\left[-\frac{\left(\mathbf{r}_2^2 - \mathbf{r}_1^2\right)^2}{r_c^4}\right], \tag{8}$$

with r_c=$(2/ka)^{1/2}$ is the coherence length, G_0=$1/H_{2m}(0)$ is coefficient and $H_{2m}(x)$ denotes the Hermite polynomial of order $2m$. Eq. (8) shows that the spectral degree of coherence is not a homogeneous function, i.e. $\mu(\mathbf{r}_1, \mathbf{r}_2) \neq \mu(\mathbf{r}_1 - \mathbf{r}_2)$; it is non-uniformly correlated. We call this class of partially coherent beams whose CSD is given by Eqs. (7) and (8) as HNUC beams. Under the condition of m=0, HNUC beams reduce to the conventional NUC beams.

Figure 1 shows the density plot of the absolute value of the DOC of the proposed HNUC beams for different values of the beam order m in the source plane with r_c=$3cm$. One finds that the number of side lobes increases as the value of the beam order m increases. We therefore have a class of non-uniformly correlated beams with distinct correlation functions.

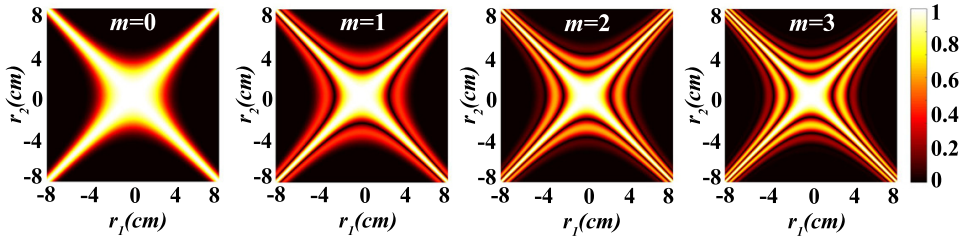

Fig. 1. Density plot of the absolute value of the DOC of HNUC beams for different values of the beam order m with r_c=$3cm$.

3. Propagation properties of HNUC beams in turbulent atmosphere

In this section, the propagation properties of HNUC beams in free space and turbulent atmosphere are investigated. Under the paraxial approximation, the propagation of a partially coherent beam from the source plane z=0 into an arbitrary plane z>0 in a turbulent medium can be described by the extended Huygens-Fresnel principle [1]

$$W(\boldsymbol{\rho}_1, \boldsymbol{\rho}_2, z) = \left(\frac{k}{2\pi z}\right)^2 \int\int_{-\infty}^{\infty} W_0(\mathbf{r}_1, \mathbf{r}_2) \exp\left[-\frac{ik}{2z}(\mathbf{r}_1 - \boldsymbol{\rho}_1)^2 + \frac{ik}{2z}(\mathbf{r}_2 - \boldsymbol{\rho}_2)^2\right] \times \langle \exp[\Psi(\mathbf{r}_1, \boldsymbol{\rho}_1) + \Psi^*(\mathbf{r}_2, \boldsymbol{\rho}_2)]\rangle \, d^2\mathbf{r}_1 d^2\mathbf{r}_2, \tag{9}$$

where $\boldsymbol{\rho}_1$ and $\boldsymbol{\rho}_2$ represent two arbitrary spatial positions in the target plane, $W_0(\mathbf{r}_1, \mathbf{r}_2)$ denotes the CSD of the beams in the source plane, and $\Psi(\mathbf{r}, \boldsymbol{\rho})$ denotes the complex phase perturbation induced by the refractive-index fluctuations of the random medium between $\mathbf{r}$ and $\boldsymbol{\rho}$. The last term in Eq. (9) can be expressed as [1]

$$\langle \exp[\Psi(\mathbf{r}_1, \boldsymbol{\rho}_1) + \Psi^*(\mathbf{r}_2, \boldsymbol{\rho}_2)]\rangle = \exp\left\{-4\pi^2 k^2 z \int_0^1 \int_0^{\infty} \boldsymbol{\kappa}\Phi_n(\boldsymbol{\kappa}) \cdot \{1 - J_0[|(1-\xi)\mathbf{P} + \xi\mathbf{Q}|\boldsymbol{\kappa}]\}\right\} d^2\boldsymbol{\kappa} d\xi, \tag{10}$$

where $\mathbf{P} = \boldsymbol{\rho}_1 - \boldsymbol{\rho}_2$, $\mathbf{Q} = \mathbf{r}_1 - \mathbf{r}_2$ and J_0 is the Bessel function of zero order and can be approximated as [1]

$$J_0[|(1-\xi)\mathbf{P} + \xi\mathbf{Q}|\boldsymbol{\kappa}] \sim 1 - \frac{1}{4}[(1-\xi)\mathbf{P} + \xi\mathbf{Q}]^2 \boldsymbol{\kappa}^2. \tag{11}$$

Optics EXPRESS

On substituting from the relation (11) into Eq. (10), we have

$$\begin{aligned}&\langle \exp\left[\Psi\left(\mathbf{r}_1,\boldsymbol{\rho}_1\right)+\Psi^*\left(\mathbf{r}_2,\boldsymbol{\rho}_2\right)\right]\rangle = \\ &\exp\left\{-\left(\frac{\pi^2k^2z}{3}\right)\left[\left(\boldsymbol{\rho}_1-\boldsymbol{\rho}_2\right)^2+\left(\boldsymbol{\rho}_1-\boldsymbol{\rho}_2\right)\cdot\left(\mathbf{r}_1-\mathbf{r}_2\right)+\left(\mathbf{r}_1-\mathbf{r}_2\right)^2\right]\int_0^\infty \boldsymbol{\kappa}^3\Phi_n\left(\boldsymbol{\kappa}\right)d^2\boldsymbol{\kappa}\right\},\end{aligned} \tag{12}$$

where $\Phi_n\left(\boldsymbol{\kappa}\right)$ is the spatial power spectrum of the refractive-index fluctuations of the turbulent atmosphere. For the simplicity of expression, we set

$$T=\int_0^\infty \boldsymbol{\kappa}^3\Phi_n\left(\boldsymbol{\kappa}\right)d^2\boldsymbol{\kappa}. \tag{13}$$

We model the turbulence using the van Karman power spectrum, which can describe Kolmogorov ($\alpha = 11/3$) and non-Kolmogorov ($\alpha \neq 11/3$) power spectrum including with inner and outer scales [29, 30]

$$\Phi_n\left(\boldsymbol{\kappa}\right)=A\left(\alpha\right)C_n^2\left(\kappa^2+\kappa_0^2\right)^{-\alpha/2}\exp\left(-\kappa^2/\kappa_m^2\right). \tag{14}$$

With this spectrum, T can be expressed in the following form [29, 30]

$$T=\frac{A(\alpha)}{2(\alpha-2)}C_n^2\left[\beta\kappa_m^{2-\alpha}\exp\left(\kappa_0^2/\kappa_m^2\right)\Gamma_1\left(2-\alpha/2,\kappa_0^2/\kappa_m^2\right)-2\kappa_0^{4-\alpha}\right], 3<\alpha<4, \tag{15}$$

where Γ_1 is the incomplete Gamma function, $\beta = 2\kappa_0^2 - 2\kappa_m^2 + \alpha\kappa_m^2$, $\kappa_0 = 2\pi/L_0$ with L_0 being the outer scale of turbulence, $\kappa_m = c(\alpha)/l_0$ with l_0 being the inner scale of turbulence, and

$$A(\alpha)=\frac{1}{4\pi^2}\Gamma(\alpha-1)\cos\left(\alpha\pi/2\right), c(\alpha)=\left[\frac{2\pi A(\alpha)}{3}\Gamma(5-\alpha/2)\right]^{1/(\alpha-5)}. \tag{16}$$

The term C_n^2 in Eq. (15) is a generalized refractive-index structure parameter with units $m^{3-\alpha}$, and $\Gamma(\cdot)$ in Eq. (16) represents the Gamma function.

By inserting from Eqs. (2) and (5) and (6) into Eq. (9), after interchanging the orders of the integrals, we obtain the formula

$$W\left(\boldsymbol{\rho}_1,\boldsymbol{\rho}_2,z\right)=\int p(v)P\left(\boldsymbol{\rho}_1,\boldsymbol{\rho}_2,v,z\right)dv, \tag{17}$$

where we define $P\left(\boldsymbol{\rho}_1,\boldsymbol{\rho}_2,v,z\right)$ as

$$\begin{aligned}P\left(\boldsymbol{\rho}_1,\boldsymbol{\rho}_2,v,z\right)=&\left(\frac{k}{2\pi z}\right)^2\int\int_{-\infty}^{\infty}V_0^*\left(\mathbf{r}_1,v\right)V_0\left(\mathbf{r}_2,v\right)\exp\left[-\frac{ik}{2z}\left(\mathbf{r}_1-\boldsymbol{\rho}_1\right)^2+\frac{ik}{2z}\left(\mathbf{r}_2-\boldsymbol{\rho}_2\right)^2\right]\\ &\exp\left\{-\frac{\pi^2k^2zT}{3}\left[\left(\boldsymbol{\rho}_1-\boldsymbol{\rho}_2\right)^2+\left(\boldsymbol{\rho}_1-\boldsymbol{\rho}_2\right)\cdot\left(\mathbf{r}_1-\mathbf{r}_2\right)+\left(\mathbf{r}_1-\mathbf{r}_2\right)^2\right]\right\}d^2\mathbf{r}_1d^2\mathbf{r}_2.\end{aligned} \tag{18}$$

Substituting from Eq. (6) into Eq. (18), after a lengthy integral calculation, one obtains

$$\begin{aligned}P\left(\boldsymbol{\rho}_1,\boldsymbol{\rho}_2,v,z\right)=&\frac{w_0^2}{2w_z^2}\exp\left[-\frac{ik}{2z}\left(\boldsymbol{\rho}_1^2-\boldsymbol{\rho}_2^2\right)\right]\exp\left[-\left(\frac{w_0^2k^2}{8z^2}+\frac{1}{3}\pi^2k^2zT\right)\left(\boldsymbol{\rho}_1-\boldsymbol{\rho}_2\right)^2\right]\\ &\times\exp\left\{-\frac{1}{w_z^2}\left|-i\left[\frac{kw_0^2}{4z}(1-2vz)-\frac{1}{3}\pi^2kz^2T\right]\left(\boldsymbol{\rho}_1-\boldsymbol{\rho}_2\right)+\left(\frac{\boldsymbol{\rho}_1+\boldsymbol{\rho}_2}{2}\right)\right|^2\right\},\end{aligned} \tag{19}$$

Optics EXPRESS

where

$$w_z^2 = \frac{w_0^2}{2}\left(1 - \frac{2vz}{k}\right)^2 + \left(\frac{\sqrt{2}z}{kw_0}\right)^2 + \frac{4\pi^2 z^3}{3}T. \tag{20}$$

We obtain the CSD of HNUC beams after propagation by evaluating the integral

$$W(\boldsymbol{\rho}_1, \boldsymbol{\rho}_2, z) = \int p(v) P(\boldsymbol{\rho}_1, \boldsymbol{\rho}_2, v, z)\, dv. \tag{21}$$

The spectral intensity of HNUC beams in the output plane is obtained as

$$S(\boldsymbol{\rho}, z) = W(\boldsymbol{\rho}, \boldsymbol{\rho}, z). \tag{22}$$

The spectral degree of coherence of HNUC beams in the output plane is obtained as

$$\mu(\boldsymbol{\rho}_1, \boldsymbol{\rho}_2, z) = \frac{W(\boldsymbol{\rho}_1, \boldsymbol{\rho}_2, z)}{\sqrt{W(\boldsymbol{\rho}_1, \boldsymbol{\rho}_1, z)\, W(\boldsymbol{\rho}_2, \boldsymbol{\rho}_2, z)}}. \tag{23}$$

We can also get the propagation properties of HNUC beams in free space by using Eqs. (19)–(23) with T=0.

We use these expressions to study the propagation properties of HNUC beams in free space and turbulent atmosphere by detailed numerical calculations. In the following calculations, we choose the beam parameters and turbulent parameters as λ=632.8nm, m=2, w_0=5cm, r_c=3cm, L_0=1m, l_0=1mm, α=11/3 and C_n^2=$10^{-15}m^{-2/3}$. For convenience, the wavelength was taken to be that of common HeNe-type laser diodes; the results presented here are qualitatively similar for optical communications wavelengths. For these parameters, the Rytov variance at d km satisfies the expression σ^2=0.056$d^{11/6}$. Figure 2 shows the density plot of the normalized intensity and the absolute value of the DOC of HNUC beams upon propagation in free space. For comparison, Fig. 3 shows the density plot of the normalized intensity and the absolute value of the DOC of HNUC beams upon propagation in turbulence. Figure 4 shows the normalized intensity on-axis of HNUC beams propagation in free space and in turbulence for different beam orders.

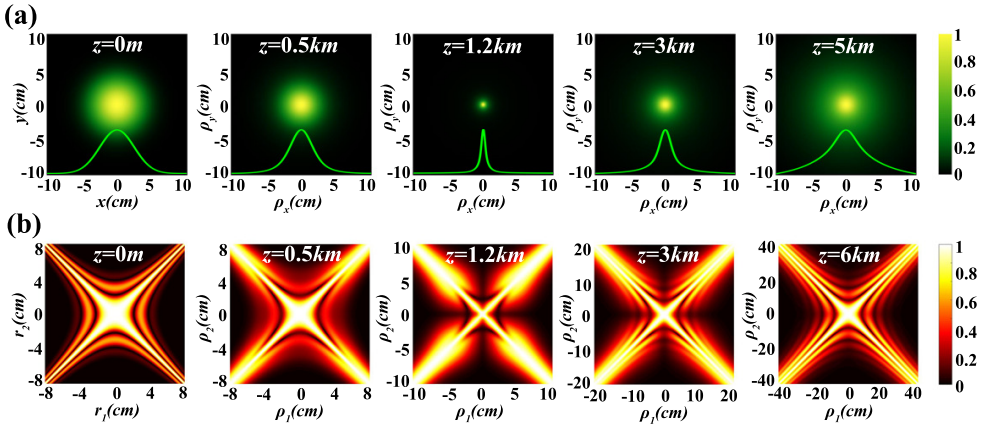

Fig. 2. Density plot of the normalized intensity and the absolute value of the DOC of HNUC beams upon propagation in free space at different distances, for the choice m = 2.

One finds from Fig. 2(a) that the distribution of the intensity of HNUC beams satisfies a Gaussian distribution in the source plane and, over short ranges, the size of the beam spot decreases with increasing propagation distance, while at long ranges, the spot size increases.

Optics EXPRESS

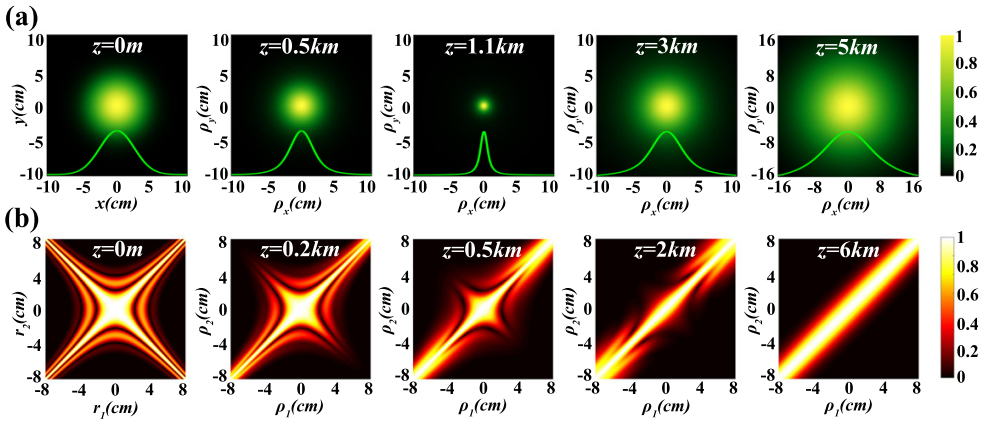

Fig. 3. Density plot of the normalized intensity and the absolute value of the DOC of HNUC beams upon propagation in turbulence at different distances, for the choice $m = 2$.

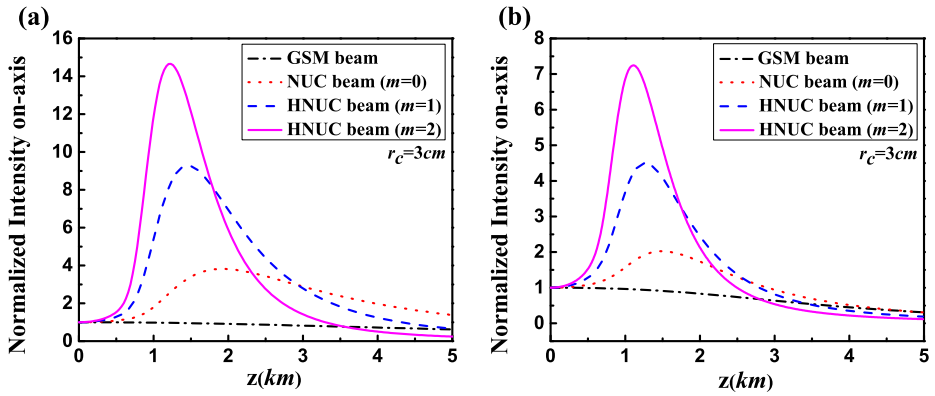

Fig. 4. Normalized intensity on-axis of HNUC beams propagation (a) in free space (b) in turbulence with r_c=3cm for different beam orders.

The beam reaches a minimum spot size, and maximum on-axis intensity, when z=1.2km. This self-focusing property is built into the definition of HNUC beams, as can be seen from Eq. (6). The curvature of each mode V_0 (**r**, v) depends on the parameter v, and the average curvature of the combined beam will depend on the mean value of $p(v)$ in Eq. (5). An HNUC beam may therefore be considered an incoherent superposition of beams with different curvatures; a conventional GSM beam in contrast may be described as an incoherent superposition of beams with different tilts.

The coherence of HNUC beams also exhibits striking effects. One finds from Fig. 2(b) that the high-coherence area of HNUC beams is confined to the center of the beam and on two diagonal lines in the source plane. When the beam is propagating in free space, the coverage of the high-coherence area in center reduces and the high-coherence area in two diagonal increases, respectively. With increasing propagation distance, the distribution of the DOC returns to the shape of the DOC in the source plane. Figure 3 shows the behavior of intensity and coherence of HNUCs in turbulence, and we find that HNUC beams still exhibit self-focusing in turbulence; however, the position of the best focus is now earlier in the propagation path, at z=1.1km. From Fig. 3(b), we find that, with increasing propagation distance, the coverage of the high-coherence area reduces gradually along one diagonal (around $\boldsymbol{\rho}_1$=−$\boldsymbol{\rho}_2$). As the propagation distance increases

Optics EXPRESS

further, the distribution of the CSD becomes spatially quasi-homogeneous, nearly constant along the diagonal lines ($\boldsymbol{\rho}_2 - \boldsymbol{\rho}_1$ = constant).

Fig. 4 shows the how the on-axis intensity depends on both propagation distance and mode order, in both free-space and turbulence. One confirms from Fig. 4(a) that the on-axis intensity of HNUC beams in free space increases over short propagation distances to a maximum, after which it decreases gradually. Furthermore, the peak value of the intensity is larger with increasing beam order, which means the self-focusing property of HNUC beams with large beam order is more dramatic. From Fig. 4(b), it can be seen that not only the peak location is closer to the source plane in turbulence, but that the peak value of the intensity of HNUC beams is smaller than that in free space. We also plot the normalized on-axis intensity of HNUC beams in turbulence for different coherence lengths [see Figs. 5(a)–5(c)]. One finds that, for HNUC beams with low coherence, self-focusing is more obvious, and the corresponding position of the peak value of the intensity is at a shorter distance. Both beam order and source coherence can therefore be used to adjust the focal position.

4. Scintillation of HNUC beams in turbulent atmosphere

According to [17, 23], the scintillation properties of PCBs can be well approximated by a finite number of their constituent modes. Therefore, we study the scintillation properties of HNUC beams in turbulence through the discretized form of Eq. (2):

$$W(\boldsymbol{\rho}_1, \boldsymbol{\rho}_2) \approx \sum_{n'=1}^{N} A_{n'}^{*}(\boldsymbol{\rho}_1) A_{n'}(\boldsymbol{\rho}_2), \tag{24}$$

where

$$A_{n'}(\boldsymbol{\rho}) = \sqrt{\triangle v}\sqrt{p(v_{n'})} V_0(\boldsymbol{\rho}, v_{n'}), \tag{25}$$

N is the number of modes, $\triangle v$ is the spacing of the modes, and $p(v_{n'})$ is the weights of these constituent modes. It is expected that HNUC beams can be synthesized by the beamlets specified by Eq. (25) when N approaches infinity. However, a small number of modes can well approximate the exact scintillation. We sample the modes in the interval $|v| \leq 2a$, and set $\triangle v = a/30$, i.e., the number modes N=61. In this case, we find the simulation is sufficient to converge to the limiting scintillation value. Thus, the scintillation index of HNUC beams is described as following:

$$\sigma^2(\boldsymbol{\rho}, L) = \sum_{m'=1}^{N}\sum_{n'=1}^{N} \langle I_{m'}(\boldsymbol{\rho}, L) I_{n'}(\boldsymbol{\rho}, L)\rangle \Big/ \left(\sum_{n'=1}^{N} \langle I_{n'}(\boldsymbol{\rho}, L)\rangle\right)^2 - 1, \tag{26}$$

here, $I'_n(\boldsymbol{\rho}, L)$ is the instantaneous intensity of the n'th mode on the target plane z=L and < > denotes the average of the realizations of turbulence. In turbulence, $\langle I_{n'}(\boldsymbol{\rho}, L)\rangle$ and $\langle I_{m'}(\boldsymbol{\rho}, L) I_{n'}(\boldsymbol{\rho}, L)\rangle$ can be derived within the framework of the Rytov approximation, given by [17, 23]:

$$\langle I_{n'}(\boldsymbol{\rho}, L)\rangle = |A_{0n'}(\boldsymbol{\rho}, L)|^2 \exp\left\{2Re\left[E_1^{n'}(\boldsymbol{\rho}, L)\right]\right\} \exp\left[E_2^{n'n'}(\boldsymbol{\rho}, L)\right], \tag{27}$$

$$\begin{aligned} &\langle I_{m'}(\boldsymbol{\rho}, L) I_{n'}(\boldsymbol{\rho}, L)\rangle = \\ &\langle I_{m'}(\boldsymbol{\rho}, L)\rangle \langle I_{n'}(\boldsymbol{\rho}, L)\rangle \exp\left\{2Re\left[E_2^{m'n'}(\boldsymbol{\rho}, L)\right]\right\} \exp\left\{2Re\left[E_3^{m'n'}(\boldsymbol{\rho}, L)\right]\right\}, \end{aligned} \tag{28}$$

where $A_{0n'}(\boldsymbol{\rho}, L)$ is the wavefield of the n'th mode in free space; it can be obtained by the generalized Collins formula [17, 23]:

$$A_{0n'}(\boldsymbol{\rho}, L) = \sqrt{p(v_{n'})} \frac{\exp(ikL)}{1 + i\alpha_{n'}L} \exp\left[-\frac{\alpha_{n'} k\rho^2}{2(1 + i\alpha_{n'}L)}\right], \tag{29}$$

Optics EXPRESS

where $\alpha_{n'} = 2/\left(kw_0^2\right) + i2v_{n'}$.

The quantities $E_1^{n'}$, $E_2^{m'n'}$ and $E_3^{m'n'}$ in Eqs. (25) and (26) are as following [23]:

$$E_1^{n'}(\boldsymbol{\rho}, L) = -\pi k^2 \int_0^L dz \int \Phi_n(\boldsymbol{\kappa}) d^2\boldsymbol{\kappa}, \tag{30}$$

$$E_2^{m'n'}(\boldsymbol{\rho}, L) = 2\pi k^2 \int_0^L dz \int \exp\left[i\left(\gamma_{m'} - \gamma_{n'}^*\right)\boldsymbol{\kappa}\cdot\boldsymbol{\rho}\right] \exp\left[-\frac{i\left(\gamma_{m'} - \gamma_{n'}^*\right)(L-z)\kappa^2}{2k}\right] \Phi_n(\boldsymbol{\kappa}) d^2\boldsymbol{\kappa}, \tag{31}$$

$$E_3^{m'n'}(\boldsymbol{\rho}, L) = -2\pi k^2 \int_0^L dz \int \exp\left[i\left(\gamma_{m'} - \gamma_{n'}\right)\boldsymbol{\kappa}\cdot\boldsymbol{\rho}\right] \exp\left[-\frac{i\left(\gamma_{m'} + \gamma_{n'}\right)(L-z)\kappa^2}{2k}\right] \Phi_n(\boldsymbol{\kappa}) d^2\boldsymbol{\kappa}, \tag{32}$$

where $\gamma_{m'} = (1 + i\alpha_{m'}z)/(1 + i\alpha_{m'}L)$ and $\gamma_{n'} = (1 + i\alpha_{n'}z)/(1 + i\alpha_{n'}L)$. $\Phi_n(\boldsymbol{\kappa})$ is the spatial power spectrum given by Eq. (14).

Now, we can calculate the scintillation index of HNUC beams numerically using Eqs. (26)–(32). In the calculations which follow, we also choose the same beam parameters and turbulence parameters as in the last section.

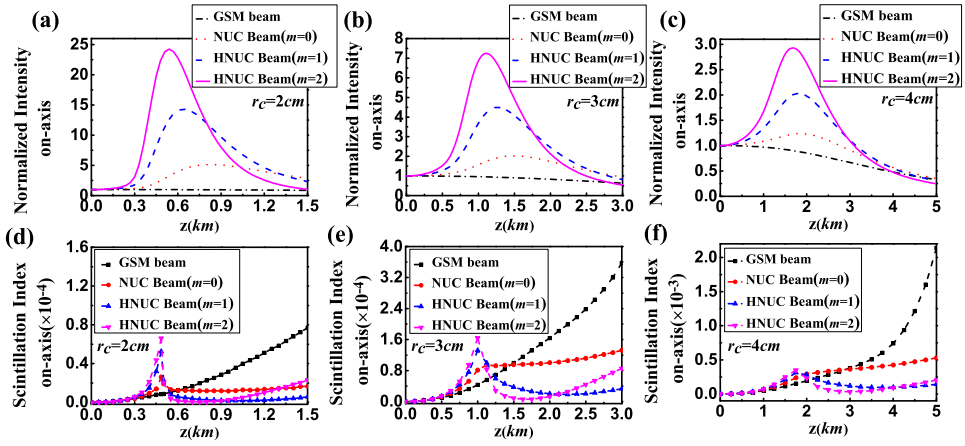

Fig. 5. Normalized intensity on-axis (a)-(c) and scintillation index on-axis (d)-(f) of HNUC beams propagation in turbulence with different beam order and different coherent length.

Normalized intensity on-axis and scintillation index on-axis of HNUC beams in turbulence with different beam order and different coherence length are shown in Fig. 5. One finds that the value of scintillation of HNUC beams increases rapidly and is significantly bigger than that of a GSM beam in the short propagation distance. But with further propagation distance, the value of scintillation of HNUC beams decreases rapidly and becomes very small, e.g., we find that in the case of r_c=2cm [Figs. 5(a) and 5(d)], after the beam propagating about 0.6km (let us define Z_c=0.6km as "Z critical"), the value of scintillation of HNUC beams is smaller than that of a GSM beam, furthermore after Z_c, the intensity of HNUC beams is much larger than that of a GSM beam. Comparing with the pink (m=2), blue (m=1) and red (m=0) line in Figs. 5(a) and 5(d), we can also find that the value of scintillation of HNUC beams is small with large beam order after Z_c, and the intensity of HNUC beams with large beam order is much larger than that of HNUC beams with small beam order and a GSM beam during Z_c. From Figs. 5(d)–(f), we find that Z_c is affected by the coherence length of HNUC beams, HNUC beams with small coherence

Optics EXPRESS

length, its Z_c will be short. So we can modulate the coherence length of HNUC beams to satisfy different requirements of propagation distance between a signal transmitter and a receiver, and we also can modulate the beam order to enhance the intensity of the beam in receiver plane and, in the meantime, reduce the negative effect from the turbulence.

Figures 6 and 7 illustrate the effects of modulating beam order and coherence length of HNUC beams in detail. We determine the peak scintillation/intensity value and peak scintillation/intensity position of HNUC beams versus the beam order with different coherence length in Fig. 6/7, respectively. From these Figs, users can determine for themselves which order and coherence length provides optimal results for their application.

We find from Fig. 6(a) that there is no peak scintillation value of HNUC with m=0 and r_c=4cm [also find it in Fig. 5(f)]. The reason is the self-focusing property of HNUC beams with high coherence is not very obvious (i.e., small change in size of beam spot), so during the beam's transmission, the influence from the turbulence is more uniform. From Figs. 6 and 7, one finds the peak value of scintillation increase with larger beam order and higher coherence; the peak value of intensity increase with larger beam order and lower coherence. The peak position of scintillation and intensity decrease with larger beam order and lower coherence.

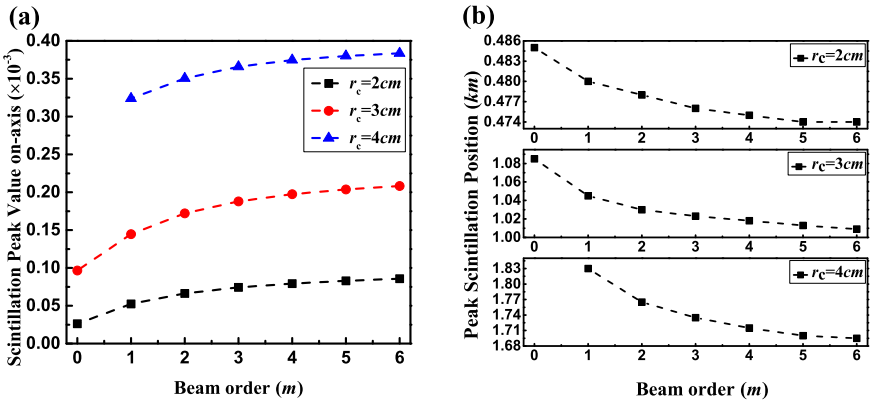

Fig. 6. Scintillation peak value (a) and scintillation peak position (b) of HNUC beams versus the beam order m different coherent length.

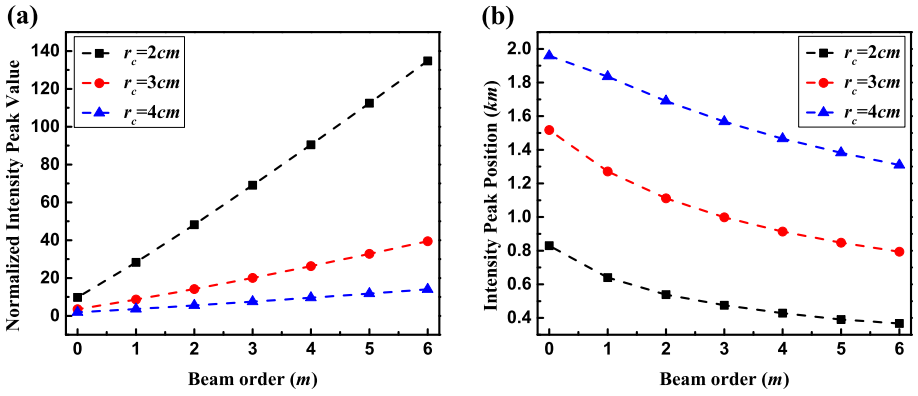

Fig. 7. Normalized intensity peak value (a) and intensity peak position (b) of HNUC beams versus the beam order m different coherent length.

Optics EXPRESS

5. Discussion

It is to be noted that the distance of peak intensity for HNUC beams is strongly correlated with the distance of peak scintillation. For example, in Figs. 5(a) and (d) one can see that the $m = 1$ and $m = 2$ beams roughly have maximum intensity and scintillation at $z = 0.5km$. Because the scintillation drops much more rapidly than the intensity, however, one can readily find distances at which the intensity is higher and the scintillation is significantly lower than a comparable GSM beam; for instance, at $z = 0.8km$. An appropriate choice of beam order and coherence parameters can therefore make HNUC beams better than GSM beams in both characteristics.

It is also worth mentioning how, at least in principle, such HNUC beams could be generated experimentally. Looking back at Eq. (2), we note that we may interpret v as a random variable with a probability distribution $p(v)$, and the function $V_0(\mathbf{r}, v)$ as a coherent Gaussian beam with a random wavefront curvature. A randomized wavefront curvature with appropriate statistics could be implemented using a programmable computer generated hologram, for example.

The class of HNUC beams introduced here therefore provide novel flexibility in controlling the intensity and scintillation of light on propagation through atmospheric turbulence. Such beams show intriguing potential for applications such as free-space optical communications, laser radar, and remote sensing.

Funding

National Natural Science Fund for Distinguished Young Scholar (11525418); National Natural Science Foundation of China (NSFC) (91750201, 1474213, 11774251); Project of the Priority Academic Program Development of Jiangsu Higher Education Institutions; China Postdoctoral Science Foundation (2016M601874); China Scholarship Council (CSC) (201706920103).